A facile method to fabricate close-packed concave microlens array on cylindrical glass

2012 J. Micromech. Microeng. 22 115026

(http://iopscience.iop.org/0960-1317/22/11/115026)

IOP PUBLISHING JOURNAL OF MICROMECHANICS AND MICROENGINEERING

J. Micromech. Microeng. **22** (2012) 115026 (7pp) doi:10.1088/0960-1317/22/11/115026

A facile method to fabricate close-packed concave microlens array on cylindrical glass

Zefang Deng, Feng Chen, Qing Yang, Hewei Liu, Hao Bian, Guangqing Du, Yang Hu, Jinhai Si, Xiangwei Meng and Xun Hou

State Key Laboratory for Manufacturing Systems Engineering & Shanxi Key Lab of Information Photonic Technique, Xi'an Jiaotong University, No 28 Xianning West Road, Xi'an, 710049, People's Republic of China

E-mail: chenfeng@mail.xjtu.edu.cn and yangqing@mail.xjtu.edu.cn

Received 20 June 2012, in final form 1 September 2012
Published 10 October 2012
Online at stacks.iop.org/JMM/22/115026

Abstract

This work presents a facile method to fabricate concave microlens arrays (MLAs) with controllable shape and high fill factor on cylindrical silica glass by a femtosecond laser-enhanced chemical wet etching process. The hexagonal and rectangular MLAs are flexibly fabricated on the silica glass cylinder with a diameter of 3 mm. The morphological characteristics of MLAs are measured by a scanning electron microscope and a laser scanning confocal microscope. The measurements show that the good uniformity and high packing density MLA structures are generated. It has also been demonstrated that the shape and size of the concave structures could be easily tuned by changing laser power and the arrangement of laser exposure spots. The convex MLAs replicated by the polymer casting method experience excellent image quality.

(Some figures may appear in colour only in the online journal)

1. Introduction

Microlens arrays (MLAs) on curvilinear surfaces have a number of applications in the fields of micromanufacture, optical sensors, lighting devices and displays systems [1–5]. For example, the concave MLAs on the cylindrical surface can also serve as roller mold for continuous and low-cost imprinting of the large-area MLAs [6]. For fabricating of MLAs, technologies like, grayscale lithography [7], thermal reflow [8], 3D diffuser lithograph [9] or ink-jet method [10] have been established. But most of these methods are planar in nature, and can hardly be used to fabricate close-packed MLAs on curved surfaces. In recent years, some new approaches, such as soft lithography [11], surface wrinkling [12], reconfigurable microtemplating technique [3], laser direct writing process [13, 14] and diamond tools manufacturing [15], have been adopted for nonplanar microfabrication. Soft lithography can be used to fabricate MLAs on curved surfaces. But the special masks used in the process would limit the packing density of the microlenses. Although reconfigurable microtemplating and surface wrinkling processes have demonstrated the ability to fabricate close-packed microlenses on spherical surfaces, the surface of the microlenses is not smooth enough to produce high-quality images. Laser direct writing and diamond tools manufacturing are maskless techniques for fabricating 2D or 3D microstructures. But these methods also have limitations in efficiency, materials and cost. It is still challenging to achieve precise and close-packed micro-optical elements onto curved surfaces.

Recently, our group has introduced the femtosecond laser-induced chemical etching (FLICE) technique to fabricate concave MLAs [16] on planar glass substrate, and high-quality MLAs have been successfully fabricated. In this paper, we propose a facile method to fabricate close-packed concave MLAs on the cylindrical silica glass by taking the advantages of the FLICE technique, coaxial adjustment and defocusing compensation processes. Uniform MLAs are achieved on cylinder glass, and their excellent optical performances were approved by high-resolution imaging. Our approach offers several advantages, such as the capacity for creating

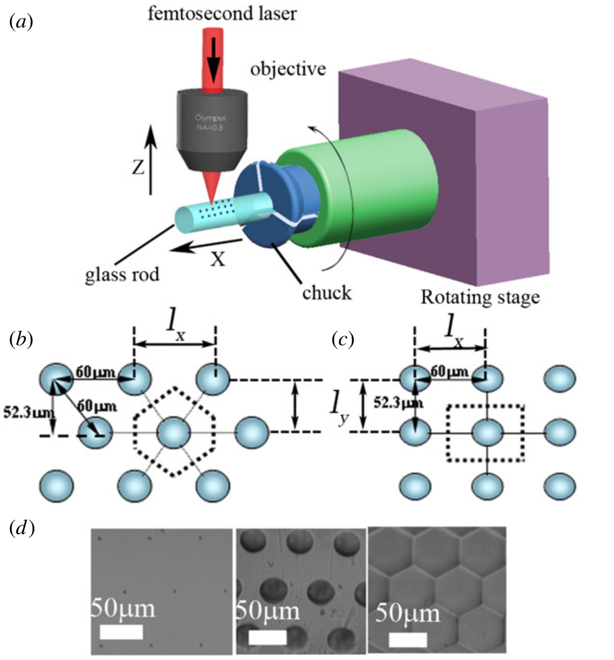

Figure 1. Illustration of the local exposure device with a rotating stage for cylindrical surface. (*a*) Laser-exposure fabricating process. (*b*) Triangular laser-exposure-spots arrangement. (*c*) Orthogonal laser-exposure-spots arrangement. (*d*) Optical microscopy images of the morphology revolution of hexagonal-arrangement exposure spots during the chemical etching process.

close-packed concave MLAs on the silica glass cylinders, facile and high efficient fabrication procedures and ease of tuning the shape and size of microlenses. To demonstrate its flexibility, various microlenses with hexagonal, rectangular and pentagonal shapes were fabricated on silica glass cylinders with a diameter of 3 mm. The 2D and 3D morphology of fabricated MLAs was measured by a scanning electron microscope (SEM) and a laser scanning confocal microscopy, respectively. Finally, convex MLAs were replicated on the planar PMMA and PDMS films by the casting process. The excellent imaging performance of the replicated MLAs demonstrates the uniformity and smooth surfaces of the MLAs.

2. Fabrication procedures

To fabricate the concave microlens arrays (MLAs) on the cylindrical silica glass surface, a laser-based two-step method was used, which is schematically depicted in figure 1. We started with a point-by-point laser exposure to create a certain arrangement spots on the cylindrical silica glass surface using a focused femtosecond (fs) laser. The laser is an oscillator–amplifier Ti:sapphire laser with the center wavelength, pulse duration and repletion rate of 800 nm, 30 fs laser and 1 kHz, respectively. The laser exposures process is schematically depicted in figure 1(*a*). The silica glass cylinder with the diameter of 3 mm was mounted on a rotary translate stage (M-037. DG, PI) by a commercial scroll chuck, which was fixed onto a 3D translate stage (DG M-126 for the *z*-axis, M-505.6G for the *x*- and *y*-axis, PI). The laser beam was normally focused onto the cylindrical silica glass surface by a 50× objective lens (NA = 0.5, Olympus). For each spot, the exposure time was controlled by a fast mechanical shutter and the laser power was tuned by a variable attenuator. The exposure time of every spot was 500 ms, and the energy of a single pulse was 3 μJ. By alternately translating and rotating the sample along the *x*-axis and the circumferential direction, respectively, triangle-arranged (figure 1(*b*)) and orthogonal-arranged (figure 1(*c*)) exposure spots were generated on the glass cylinder surfaces. To achieve the close-packed pattern, the exposure spots were equidistantly distributed on the cylindrical surface. The line distance in the circumferential direction, l_y, was set at 52.3 μm (the rotation angle of each step was 2°). The interspace between two spots along the *x*-axis direction was 60 μm, which is calculated by the following equation:

$$l_x = \frac{2l_y}{\sqrt{3}}.$$

Compared with planar glass substrate, fabrication on cylinder glass would cause defocusing problem heavily, which resulted in the fluctuation of the laser energy density between the exposure spots. In order to get uniform microlenses, each spot should be irradiated under the same laser conditions. Here, some strategies were adopted: (1) the rotary translation stage was regulated parallel to the horizon plane to guarantee the direction of the incident laser strictly perpendicular to the cylindrical surface; (2) the coaxial fixed chuck for the sample was specially designed and made to ensure the incident laser beam passed through the central axis of the cylinder glass during movement, and it was carefully calibrated onto the rotary stage, which ensures that the rotating off-axis distance was less than 5 μm; (3) with monitoring by an optical microscope system equipped with a CCD camera, an extra defocusing compensation was implemented by translating the sample along *z*-axis direction during the laser exposure process.

After the laser exposures, the sample was immersed in 5% hydrofluoric (HF) acid solution (diluted by deionized water) at room temperature. The morphology revolution of the hexagonal MLAs during chemical wet etching is schematically depicted in figure 1(*d*). The formation of the concave microstructures is associated with the fs laser-induced modifications inside the silica glasses, which will increase the local etching rate. During this process, the concave structures expanded homogeneously and progressively formed circular patterns. Then, the adjacent circular structures ‘squeeze’ with each other to form the hexagonal-shaped MLAs. When the smooth concave surfaces were successfully fabricated, the sample is cleaned by deionized water and dried.

3. Results and discussions

3.1. The morphology of the microlens

The hexagonal and rectangular MLAs were fabricated by using the laser-enhanced chemical etching with different arranged exposure spots. Figures 2(*a*) and (*d*) show the SEM images of the fabricated microstructures. The 3D and 2D profiles of the microlenses were measured by a laser scanning confocal

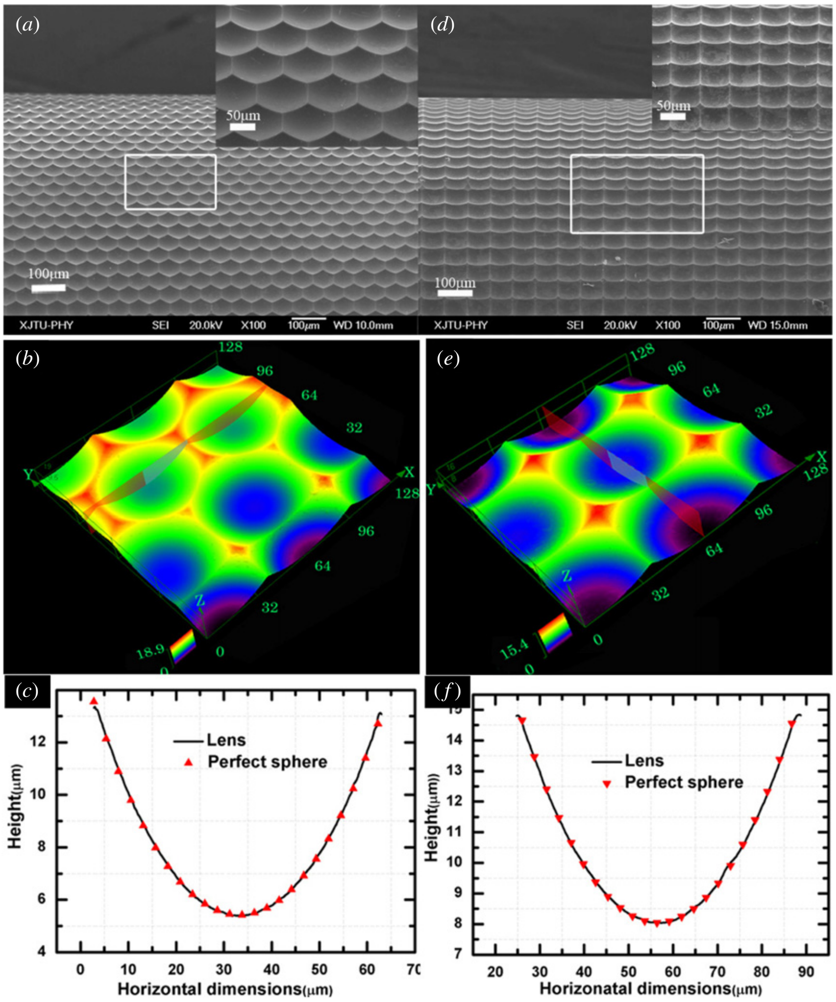

Figure 2. The morphology of microlenses. (*a*), (*d*) The SEM images of the hexagonal and rectangular microlens arrays, respectively. (*b*), (*e*) The 3D morphologies of hexagonal and rectangular microlens arrays, respectively. (*c*), (*f*) The cross-sectional profile of the fabricated (solid line) hexagonal and rectangular microlens and the theoretical sphere surface (dotted line).

microscopy (LSCM, Olympus LEXT OLS4000), and the results are shown in figures 2(*b*), (*c*) and (*e*), (*f*). The length (D) and the height (h) of the hexagonal microlens are 61.5 μm and 7.26 μm, respectively. The focal length of the microlenses can be calculated by the following equation:

$$f = \frac{R^2 + h^2}{2h(n-1)} - h(n-1) \tag{1}$$

where R and h are the radius and height of a microlens, respectively, and n is the refractive index of silica glass. Considering $n = 1.51$, $R = 30.75$ μm ($R = D/2$), we obtain the focal length of hexagonal microlens f_1 as 131.1 μm. For the rectangular microlens, the length (D) and the height (h) are 61.4 μm and 7.19 μm, respectively. The focal length f_2 of the rectangular microlens is 131.9 μm, calculated from the equation (1). In addition, the cross-sectional profiles (solid lines) of the hexagonal- and rectangular-shaped microlenses are close to the theoretical circular curves (dotted lines), as shown in figures 2 (*c*) and (*f*), respectively, demonstrating the spherical surfaces of the concave microlenses fabricated by our approach.

3.2. Formation mechanism of the concave microlens

The self-formation of the concave microstructures can be contributed to the laser-induced material modifications. To study the formation mechanism, the diameter of a concave microlens during the chemical etching is measured at different etching times, as shown in figure 3(*a*). The inset in figure 3(*a*) shows the morphology of fs laser-induced damage crater, which was ablated by a 3 mW fs laser with exposure time of 500 ms. The laser-induced crater with a diameter of 4 μm is produced by the Coulomb explosion triggered by the avalanche ionization on the picosecond timescale [17, 18]. Within a few nanoseconds after the explosion, strong pressure/stress wave or shockwave generated and expanded from focal volume, causing a series of material modifications such as nano-cracks and high refractive index structures. These laser-induced modifications would accelerate local chemical wet etching rate [19, 20]. After the first 10 min of the etching, the diameter of the concave microlens reached to about 45 μm; the average etching rate at this period are about 4 μm min^{-1}. This average etching rate then decreases to about 0.35 μm min^{-1} in the following 40 min. The formation of closed-packed MLAs can be explained as

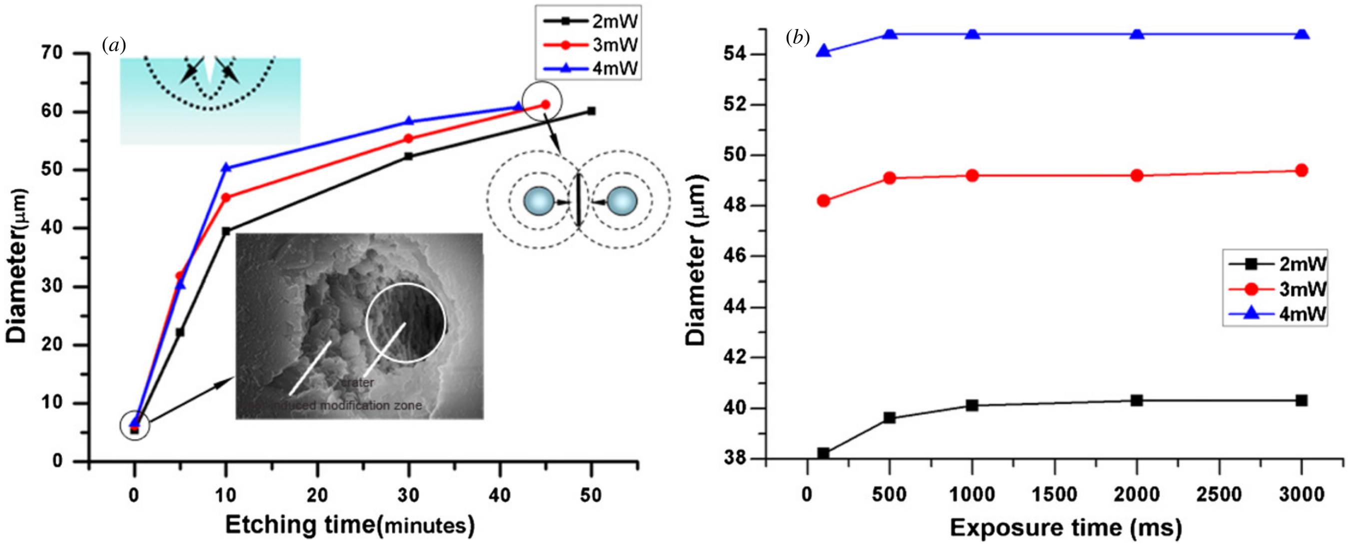

Figure 3. (*a*) The graph of the diameter increase along with time in different laser power and the basic forming process of microlens during chemical etching. (*b*) The relationship between the laser exposure time and the diameter of microlens.

follows: when immersed in the 5% HF acid solution, the modification materials around the crater, which diameter is 45 μm, was rapidly etched out and formed a concave structure. Subsequently, two adjacent concave structures expand homogeneously, contact with each other and finally form a straight boundary. Therefore, the close-packed MLAs can be easily obtained by the chemical etching process.

3.3. Control of the size and shape of the microlenses

The flexibility in controlling the size and shape of microlens was demonstrated by fabricating MLAs with different shapes using fs-laser-enhanced wet etching. The range of the laser-modified materials is closely associated with the laser power, and the size of the wet-etched concave microlenses can be consequentially influenced by it. To study the power dependence of the size of concave microlenses, different laser exposure powers are applied to produce MLAs on silica glass cylinders. In the experiments, the laser power ranges from 2 mW to 4 mW. The results of the diameter of the formed concave microlenses (figure 3(*a*)) indicate that the diameters of the concave structures are closely related to the laser power and it will increase with the increase of laser power. Moreover, the relationships between laser exposure time and the diameters of microlens are also investigated. By changing the laser exposure time from 10 ms to 3000 ms at different laser power (2 mW, 3 mW and 4 mW), different sizes of concave microlenses are obtained. The sample is then etched by a 5% HF solution for 20 min. Figure 3(*b*) shows the influence of laser exposure time on the diameter of the microlens.

To fabricate various microlenses with different shapes, we changed exposure spots arrangement in the laser exposure process. Figure 4 shows that pentagonal and hexagonal, hexagonal and rectangular MLAs are successfully fabricated with different exposure arrangement. Moreover, though the size of microlens can be controlled by designing the interval between adjacent laser exposure spots, the mechanical error of the translation stages and the power fluctuation of laser may caused a tiny fluctuation. Compared to the designed length of a single microlens, 60 μm, the deviation of the length of fabricated microlens, 61.5 μm, is just less than 5%.

The fill factor and surface smoothness of microlens are significant conditions to impact the overall light efficiency. In order to collect the maximum amount of light, the area of microlenses should be as close to 100% as possible. Most of the literature related to fabrication of microlenses discussed only round geometrical microlenses [5, 15, 21]. Assuming that there are no gaps between these round microlenses, the maximum fill factor for a round MLAs in orthogonal and hexagonal arrangement are 78% and about 91%, respectively. The shape of fabricated microlenses in figures 2(*a*) and (*d*), demonstrating good uniformity, smooth surface and high fill factor, are hexagon and rectangle, respectively. Both of them have a larger fill factor than the round MLAs, and reach a maximum fill factor of 100%. In addition, the surface morphology of the hexagonal microlenses was measured using an atomic force microscope (AFM). The average surface roughness value, Ra = 24 nm, which was tested in an area of $15 \times 15\ \mu m^2$ at the bottom of a concave microlens. The nanometer-scaled surface roughness is essential for microlenses to reduce the light scattering and achieve high-resolution imaging performances.

3.4. Replication of the MLAs

Serving the MLAs as a molding template, the convex MLAs were replicated into a PMMA film. The cylindrical mold was dipped into a liquid mixture of PMMA and chloroform with a weight ratio of 1:10, and suspended in air at room temperature for 2 h. When it dried, we peeled off the PMMA thin film. In the replication process, the demolding process will determine the quality of MLAs. Thereby, to ensure the consistency and surface smoothness of replicated MLAs, the sample covered with PMMA is peeled off in deionized water with an ultrasonic bath. To facilitate the observations, the PMMA film

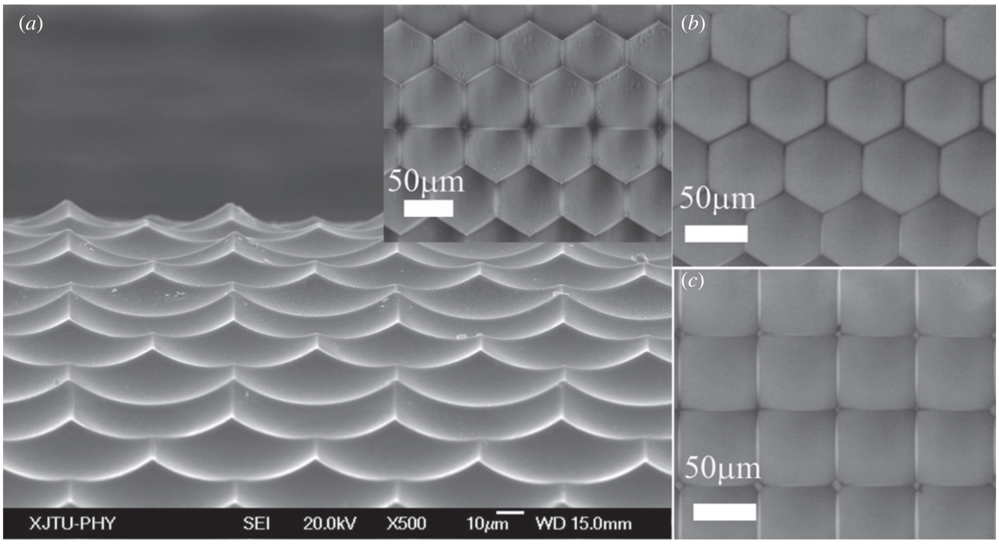

Figure 4. (*a*) The SEM and optical microscopy (OM) images of pentagonal and hexagonal MLAs. The OM images of (*b*) hexagonal and (*c*) rectangular MLAs.

replica was unfolded by two pieces of glass slides. Increasing temperature and the mass fraction of the PMMA solution can improve replication rate. But if the temperature is over 40 °C or the mass fraction of the PMMA solution is greater than 15%, it will dramatically degrade the quality of replicated MLAs. After optimization, we found that mass fraction of 10% and 20–30 °C temperature range are suitable to obtain high-quality replicated MLAs.

The 3D morphology of the replicated convex hexagonal MLAs was measured by the optical microscopy and LSCM. Figure 5(*a*) shows that the replicated MLAs have a good uniformity and low surface roughness. Figures 5(*b*) and (*c*) show the 3D morphology and cross-section of the replicated hexagonal MLAs, respectively. The length of the hexagonal convex microlens, D, is 62.1 μm, and the height of the microlens, h, is 6.73 μm. Moreover, considering the refractive index of PMMA $n = 1.49$, we can calculate its focal length $f = 149.7$ by equation (1). And the replicated microlens has the deviation of approximately 8% in height, and of 1.1% in length.

To demonstrate the imaging properties of the replicated MLAs, a projection experiment was performed on the replicated convex MLAs. Firstly, the MLAs were positioned on a sample stage of the optical microscope. Next, the projection template with a transparent letter 'A' on it is placed between the tungsten light source and convex MLAs. Then, the miniaturized letters were projected onto the focal plane of the MLAs and imaged through objective lens of the microscope. Finally, a CCD camera was used to catch the images. A hexagonal and rectangular array of images 'A' were observed by a 10 × objective lens on the MLAs. Figure 6 shows that every microlens can form sharp images, demonstrating the perfect imaging properties of the MLAs.

Moreover, we took a glass cylinder with concave MLAs as a replication mold for casting convex MLAs using poly dimethylsiloxane (PDMS). The glass cylinder with hexagonal concave MLAs was dipped in the liquid poly PDMS and

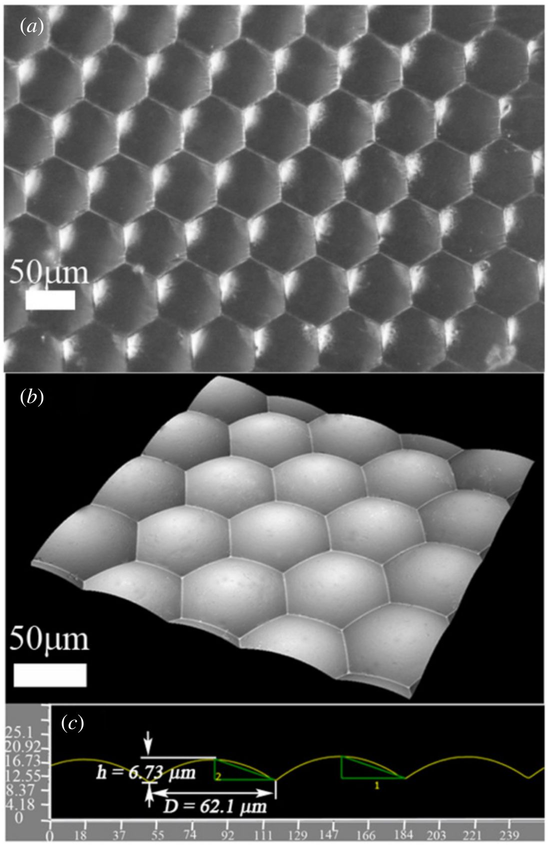

Figure 5. (*a*) The optical microscopy (OM) images of replicated hexagonal MLAs. (*b*) The morphology of replicated convex hexagonal microlenses. (*c*) The section profile of the hexagonal microlenses. The convex hexagonal microlens has the length of 62.1 μm, and the height of 6.73 μm.

then heated the sample at 75°C for 60 min. After the PDMS film was cured, we peeled the film. For the reason of the plastic property of PDMS, the film will be cylindrical, and the replicated convex MLAs distribute on the concave cylindrical

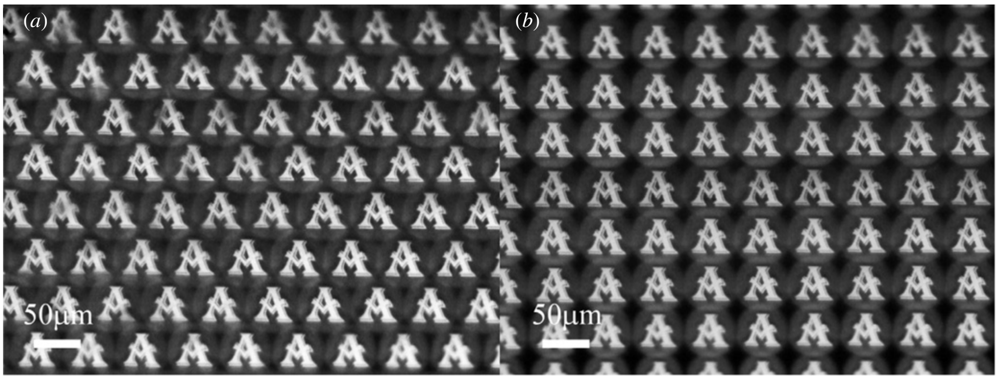

Figure 6. The images captured by the optical microscope system for the replicated (*a*) hexagonal and (*b*) rectangular microlens array.

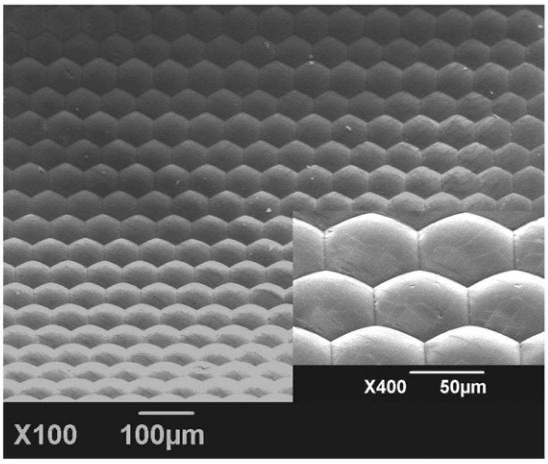

Figure 7. The SEM images of replicated convex MLAs on the concave cylindrical surface.

surface. Figure 7 shows the SEM images of the convex MLAs on concave cylindrical surface, and it visually demonstrates a good uniformity.

4. Conclusions

In summary, we have demonstrated a simple method to fabricate concave microlenses on the nonplanar surfaces using the femtosecond laser-enhanced chemical wet etching. Hexagonal, rectangular and pentagonal and hexagonal microlenses were fabricated on a glass cylinder, and high-quality convex microlenses were successfully replicated. The advantages of this technique, such as the ability to create close-packed microlenses with smooth surface, facile and high efficient fabrication procedures and ease of tuning the shape and size of microlenses, have also been demonstrated in the experiments.

Acknowledgment

This work is supported by the National Science Foundation of China under the grant no 61176113, National High Technology R&D Program of China under the grant no 2009AA04Z305 and the Fundamental Research Funds for the Central Universities.

References

[1] Li L and Yi A Y 2009 Microfabrication on a curved surface using 3D microlens array projection *J. Micromech. Microeng.* **19** 105010

[2] Liu S-J and Chang Y-C 2007 A novel soft-mold roller embossing method for the rapid fabrication of micro-blocks onto glass substrates *J. Micromech. Microeng.* **17** 172–9

[3] Jeong K-H, Kim J and Lee L P 2006 Biologically inspired artificial compound eyes *Science* **312** 557–61

[4] Kim J-J, Chae S and Feong K-H 2010 Micropatterned single lens for wide-angle light-emitting diodes *Opt. Lett.* **35** 823–5

[5] Rim S-B, Catrysse P B, Dinyari R, Huang K and Peumans P 2008 The optical advantages of curved focal plane arrays *Opt. Express* **16** 4965–71

[6] Jiang L-T, Huang T-C, Chiu C-R, Chang C-Y and Yang S-Y 2007 Fabrication of plastic microlens arrays using hybrid extrusion rolling embossing with a metallic cylinder mold fabricated using dry film resist *Opt. Express* **15** 12088–94

[7] Wu M-H, Park C and Whitesides G M 2002 Fabrication of arrays of microlens with controlled profiles using gray-scale microlens projection photolithography *Lagnmuir* **18** 9312–8

[8] Lin C-P, Yang H and Chao C-K 2003 Hexagonal microlens array modeling and fabrication using a thermal reflow process *J. Micromech. Microeng.* **13** 775–81

[9] Chang S, Yoon J-B, Kim H, Kim J-J, Lee B-K and Shin D H 2006 Microlens array diffuser for a light-emitting diode backlight system *Opt. Lett.* **31** 3016–8

[10] Danzebrink R and Aegerter M A 2001 Deposition of optical microlens array by ink-jet processes *Thin Solid Films* **392** 223–5

[11] Childs W R and Nuzzo R G 2004 Patterning of thin-film microstructures on non-planar substrate surfaces using decal transfer lithography *Adv. Mater.* **5** 1323–7

[12] Chan E P and Crosby A J 2006 Fabricating microlens arrays by surface wrinkling *Adv. Mater.* **18** 3238–42

[13] Xie Y, Lu Z, Li F, Zhao J and Weng Z 2002 Lithographic fabrication of large diffractive optical elements on a concave lens surface *Opt. Express* **10** 1043–5

[14] Radtke D, Duparré J, Zeitner U D and Andreas 2007 Laser lithographic fabrication and characterization of a spherical artificial compound eye *Opt. Express* **15** 3067–77

[15] Scheiding S, Yi A Y, Gebhardt A, Li L, Risse S, Eberhardt R and Tünnermann A 2011 Freeform manufacturing of a microoptical lens array on a steep curved substrate by use of a voice coil fast tool servo *Opt. Express* **19** 23938–51

[16] Chen F, Liu H, Yang Q, Wang X, Hou C, Bian H, Liang Weiwei, Si J and Hou X 2010 Maskless fabrication of

concave microlens arrays on silica glasses by a femtosecond-laser-enhanced local wet etching method *Opt. Express* **18** 20334–43

[17] Roeterdink W G, Juurlink L B F, Vaughan O P H, Diez J D, Bonn M and Kleyn A W 2003 Coulomb explosion in femtosecond laser ablation of Si(1 1 1) *Appl. Phys. Lett.* **79** 4190–2

[18] Gattass R R and Mazur E 2008 Femtosecond laser micromachining in transparent materials *Nature Photoni.* **2** 219–25

[19] Sakakura M, Terazima M, Shimotsuma Y, Miura K and Hirao K 2007 Observation of pressure wave generated by focusing a femtosecond laser pulse inside a glass *Opt. Express* **15** 5674–86

[20] Bellouard Y, Said A, Dugan M and Bado P 2004 Fabrication of high-aspect ratio, micro-fluidic channels and tunnels using femtosecond laser pulses and chemical etching *Opt. Express* **12** 2120–9

[21] Park B G, Choi K, Jo C J and Lee H S 2011 Micro-lens-on-lens array *Soft Matter* **8** 1751–5